Preliminary design of dust lifting and transport in the martian General Circulation Model.

François Forget and Frédéric Hourdin

January 15, 1998
Technical note for ESA contract 11369/95/NL/JG,
Work Package 4

Contents

1 Introduction

The dust carried by the Martian atmosphere strongly affects the thermal structure through its radiative effects, and, in turn, the atmosphercic circulation. The amount of airborne dust is one of the most variable components of the Martian environments, with a strong seasonal cycle, considerable year to year variations and large spatial variations.

In the GCMs that have been used to produce the Martian database for ESA, the amount of dust lifted in the atmosphere has been simply prescribed on the basis of the few available observations. Prescribing the dust may sometimes lead to unrealistic results, especially for the periods when the atmosphere is dust laden. From an engineering point of view, these periods are of particular importance since they corresponds to the most extreme conditions for a spacecraft, with strong winds below 50 km (dust storms) and a denser atmosphere abaove (the dust enhance the meridional Hadley circulation which leads to a strong adiabatic cooling of the upper atmosphere in the summer hemisphere and in the tropics). Also, prescribing the dust hinders the estimation of the interranual variability of the Martian environment, since this variability is also controlled by the dust cycle fluctuations.

To improve knowledge of the dust cycle, and better simulate the related changes in the environmental conditions for the future missions to Mars, we are developping a version of the general circulation model in which the various aspect of the dust cycle are parametrised :

- Dust lifting by the general circulation or, alternatively, by local dust devils.
- Vertical turbulent mixing of the dust, especially in the planetary boundary layer.
- Vertical mixing by atmospheric convection
- Transport by the general circulation
- Gravitational sedimentation
- CO_2 or H_2O condensation induced sedimentation (scavenging).

This document discusses these various aspects and describes parametrizations that have been designed to simulate them. In practice, a new prognostic variable have been added to the traditional general circulation model variables : q, which is the dust mixing ratio in the atmosphere (in kg of dust per kg of atmosphere).

2 Dust lifting

2.1 Lifting by the general circulation winds predicted by the GCM

When wind blows accross a surface covered by loose particles, kinetic energy is transferred to the surface through shear stress. Thus the lifting of dust by the near surface winds is primarily a function of the wind stress τ(in N m^{-2}) on the surface. To first order, it is given by :

$$\tau = \rho {u^*}^2 \tag{1}$$

where ρ is the air density and u^* the friction velocity. In the current version of the GCM, u^* is deduced from the wind velocity in the first layer (at height z_1 above the surface) :

$$u^* = \sqrt{C_d}\, u(z_1) \tag{2}$$

with :

$$C_d = (\frac{k}{\ln \frac{z}{z_0}})^2 \tag{3}$$

where k is the Von Karman constant ($k = 0.4$), z_0 is the roughness coefficient ($z_0 = 0.01$ m in the GCM). Note that C_d does not depend on the near surface temperature profile because of the small depth of the first layer in the model ($z_1 \sim 4$ m). It has been assumed that the wind profile in the first meters above the surface is logarithmic.

2.1.1 *Threshold stress*

The minimal wind stress required to initiate particle motion primarily depends on the particles size, which in turn controls the aerodynamic properties of the particles and the interparticle forces. The quantitative determination of this threshold stress is not straightforward. On Mars, analytical models (White, 1979) and wind tunnel simulations (Greeley et al., 1980, 1994) have shown that the particle size moved by lowest winds is about 100 μm in diameter. Depending on the assumed surface pressure and temperature, the threshold wind stress was found to be about 0.03-0.04 N m^{-2}.

Comparison with Viking observations : These values correspond to wind velocities at 1.6 meters of the order of 30 m s^{-1} for a surface roughness like at the Viking Lander site. The strongest winds measured by the Viking Landers during the second global dust storm (peak gusts of 28 m s^{-1} at 1.6 m) did not reach threshold conditions, but indeed came close: movement did occur in sand piles placed on the top of the Lander, but no alteration was observed to occur on the surface. Stronger wind only occured two years later, during the third winter of Lander 1 observations, when bright dust deposits left by earlier dust storms were eroded and when piles of soil artificially created on the ground were modified and in some case removed [Arvidson et al.(1983)]. Unfortunately, the wind sensor was not operating at that time. All these observations are consistent with the experimental and theoretical analyses described above.

The 100-μm particles are lifted from the surface at a heigth of some tenth of centimeters, but as the drag is not sufficient to exceed the weigth, they are carried downwind back to the surface (**saltation**). Smaller particles requires stronger wind to be lifted, (but much lower winds can keep them aloft once lifted). In particular, suspended dust on Mars, thought to be of the order of one microns in diameter, requires winds way above the maximum winds observed or predicted on Mars to be lifted (surface stress $\tau > 0.3$ N m^{-2}). This is true for dust that settled on smooth, homogeneous surfaces. However, experiments have shown that micron-sized particles on top of small pebbles can be removed by lower, more realistic, friction velocities : $u^* \sim 1.3$ m s^{-1} with $P_s = 10$ mb and $T = 300$ K, corresponding to $\tau \sim 0.03$ N m^{-2} (Greeley et al., 1994) . The threshold velocities is also lowered by 25 to 40% when the atmosphere is unstable, as occur during surface heating [White and Greeley(1989)].

In fact, it is likely that larger, saltating sand grains can dislodge the micron-sized particles to set them into suspension, as it commonly occurs on Earth (**sand-blasting**). Within this context, initiation of entrainment for these particles could start as soon as 100-μm particles are lifted ("impact threshold"), but only if such particles are available.

Choice for the model : Based on these considerations, we have assumed that dust lifting would start for threshold stress τ_t around 0.03-0.04 N m^{-2} , corresponding to the minimum stress able to initiate movement of at least $\sim 100\mu$m particles on the surface and probably fine ($< 10\mu$m) particles if they are on top of pebbles, for instance. In his own experiment recently performed with the NASA Ames model, Jim Murphy has used $\tau_t = 0.0225$ N m^{-2}. However, he is now considering that this value might be too low (Murphy, personnal communication, 1997). Clearly, τ_t is a parameter that will have to be tuned for the dust lifting model.

2.1.2 *Horizontal fluxes*

The horizontal flux of saltating grains can be estimated from physical considerations. For instance, if one assumes that, above the erosion threshold, the wind momentum is transfered to the surface by the saltating grains, one can show that the horizontal flux is proportional to a power of 3 of the wind friction velocity. On the basis of such considerations, many expressions have been suggested in the litterature. In particular, White (1979) derived an theoretical expression suitable for Mars conditions. This expression was later found to be the most reliable to account for the natural and wind tunnel simulations even for the terrestrial case. It is now used in state of the art dust emission scheme for Earth model (e.g. Marticorena and Bergametti, 1995). Thus, we have chosen to keep this expression in our model to compute the near surface horizontal dust flux G (kg m^{-1} s^{-1}) as a function of friction velocity :

$$G = 2.61 \, \frac{\rho}{g} \, (u^* - u_t^*)(u^* + u_t^*)^2 \tag{4}$$

where u_t is the threshold friction velocity computed from the prescribed theshold stress τ_t using Eq. 1 as a function of surface pressure and temperature. 2.61 is an empirical constant valid on Earth as on Mars, determined from wind tunnel tests. A sensitivity study has shown this constant to be stable over a wide range of different conditions (White, 1979, Greeley, 1994b)

2.1.3 *Vertical fluxes*

The vertical flux F (kg m^{-2} s^{-1}) is composed of the finest particles setting in suspension from the saltation layer and able to be long range transported. Thus, this is the flux which of interest for our parametrization. Clearly, F is a function of the horizontal flux G. There have been many theoretical and empirical studies to relate the two fluxes. Most recent studies have shown that the ratio F/G does not depends upon the wind friction velocity (Shao et al., 1993). . For instance, Marticorena and Bergametti (1995) used a ratio uniquely depending on the capacity of the soil to provide fine particles (in practice, the percentage of clay). On Mars, we have chosen to use a constant ratio :

$$F = \alpha G \tag{5}$$

α is a second tunable parameter. According to the terrestrial studies mentionned above, α should range between 10^{-1} and 10^{-3} m^{-1}. Such values are supported by preliminary studies performed with the GCM.

2.1.4 *Implementation in the GCM.*

In practice, we have included the dust lifting parametrization in the vertical diffusion scheme (see below). The vertical fluxes of dust is taken into account as a surface boundary conditions. If $u^* > u_t^*$, the dust mixing ratio in the first layer $q(1)$ is increased by :

$$\begin{aligned}
\frac{\partial q(1)}{\partial t} &= F \frac{g}{\delta\sigma_1 p_s} && (6)\\
&= \frac{2.61\alpha}{\delta\sigma_1 R T_s}\,(u^* - u_t^*)(u^* + u_t^*)^2 && (7)
\end{aligned}$$

Where p_s and T_s are the surface pressure and temperature, $\delta\sigma_1$ is the thickness of the first model layer in $\sigma = p/p_s$ coordinates, R is the gas constant on Mars ($R \simeq 190$ J kg^{-1} K^{-1}), g gravity (g=3.73 N kg^{-1}).

2.2 Lifting by dust devils

Dust devils form due to convection in an atmosphere with a superadiabatic lapse rate. They preferencially accur over hot surface. They may be an effective mechanism for lifting dust (It is often the case on Earth) Some dust devils were discover on Viking Orbiter Images (Thomas and Gierash 1985), mostly close to the subsolar point in the summer afternoons, and some small one were recorded in the meteorological data of the Viking Lander (Ryan and Lucich, 1983) and Pathfinder.

Such features are too small to be represented in the GCM. However, in term, we will build a simple parametrisation of this lifting process by creating a source of dust when the GCM predicts a very unstable lower atmosphere, (see section 3.2). We will then conduct sensitivity studies with or without this parametrisation in order to asses its relevance to reproduce the available observations.

Thomas and Gierasch(1985); Ryan and Lucich(1983)

3 Vertical mixing of dust by subgrid scale dynamical processes

3.1 Turbulent mixing

Just like heat and momentum, dust is transported by subgrid scale turbulence, mainly in the planetary boundary layer. In the model, we have accounted for this effect in a similar manner than what is done for heat and momentum, based on the implicite numerical resolution in σ coordinates of the classical diffusion equation :

$$\frac{\partial q}{\partial t} = \frac{1}{\rho} \frac{\partial}{\partial z} \rho K_z \frac{\partial q}{\partial z} \tag{8}$$

where the turbulent mixing coefficient K_z is computed as described in the "Detailed design document for the martian atmospheric GCM" previously suplied to ESA.

3.2 Convection

The mixing of dust by convection is done in a similar way than for momentum in the convective adjustment scheme : if an unstable profile is produced by the model ($\partial\theta/\partial z < 0$, with θ potential temperature), an adiabatic profile is immediately restored with a simple energy conserving scheme. The corresponding exchange of dust is linked to the air mass fluxes involved in the convection which cannot be estimated with such a simple scheme. Rather than completly mixing the dust particles through the depth of the unstables layers, only a fraction $\alpha < 1$ of the mesh is mixed. α is arbitrarily computed from the initial instability which is estimated from the relative enthalpy exchange necessary to restore the adiabatic profile $\overline{\theta}$ from the initial profile θ.

$$\alpha = \frac{\int \left|\overline{\theta} - \theta\right| \rho dz}{\int \theta \rho dz} \tag{9}$$

4 Transport by the general circulation

The numerical transport scheme used in our model is a "Van-Leer I" finite volume transport scheme (Van-Leer 1977) which has recently been implemented in the LMD GCM by team member F. Hourdin for martian and terrestrial application (Hourdin and Armengaud, 1997). Here we describe the principle and the performance of this scheme.

4.1 Scheme description

The transport of dust in the atmosphere is controlled by the continuity and dust conservation equations,

$$\frac{\partial \rho}{\partial t} + \mathrm{div}\,(\rho V) = 0 \tag{10}$$

$$\frac{\partial \rho q}{\partial t} + \mathrm{div}\,(\rho q V) = 0 \tag{11}$$

where ρ is the air density, q the dust mixing ratio and V the velocity field. integration on the volume of a polyhedron with N faces (in our 3D case, $N = 6$) leads to the following formulation :

$$\frac{\partial m}{\partial t} = \sum_{n=1}^{N} U_n \tag{12}$$

and

$$\frac{\partial qm}{\partial t} = \sum_{n=1}^{N} F_n \tag{13}$$

where m is the total air mass inside the polygone, q is the mean dust mixing ratio in the same volume, and U_n and F_n are the mass and dust inward fluxes for face n respectively. This formulation leads to conservative schemes as long as the same flux is used for the upstream and downstream volumes.

4.1.1 *1-Dimensional derivation*

In one dimension, and after integration over one time step, Eq. 12 and Eq. 13 just read

$$\delta_t(m)_i = U_{i-1/2} - U_{i+1/2} \tag{14}$$

and

$$\delta_t(qm)_i = F_{i-1/2} - F_{i+1/2} \tag{15}$$

where indices correspond now to position on the x axis, δ_t represents the finite difference in time, and $U_{i+1/2}$ and $F_{i+1/2}$ are the mass and dust transfers across the interface $i + 1/2$ during one time-step (fluxes integrated in time). $F_{i+1/2}$ can be rewritten as the product of the mass transfer $U_{i+1/2}$ by the mean dust mixing ratio $\hat{q}_{i+1/2}$ corresponding to the air crossing the interface (notations are illustrated in Fig. 1).

With these notations, the new value of q and m after one time step are simply

$$q_i^* = \left(q_i m_i + U_{i-1/2}\hat{q}_{i-1/2} - U_{i+1/2}\hat{q}_{i+1/2}\right)/m_i^* \tag{16}$$

and

$$m_i^* = m_i + U_{i-1/2} - U_{i+1/2} \tag{17}$$

The key problem to compute transport is clearly the estimation of $\hat{q}_{i+1/2}$, which depends on the unknown sub-grid scale ditribution.

Several methods have been suggested to approximate $\hat{q}_{i+1/2}$. One simple and widely used solution is to assume that the dust distribution inside the mesh is constant, in which case $\hat{q}$ is just the upstream value of q ($\hat{q}_{i+1/2} = q_i$ if $U_{i+1/2} > 0$ and q_{i+1} otherwise). Although computationally very cheap, this so-called "up-stream" or "Godunov" scheme suffers from a very large numerical diffusion.

The solution chosen here (Van-Leer I hereafter) is to assume that the dust varies linearly as a function of mass with a slope $(\delta q)_i = q_{i+1/2} - q_{i-1/2}$ where $q_{i\pm1/2}$ is the dust mixing ratio extrapolated at the mesh boundary (see Fig. 1 for illustration).

Then $\hat{q}_{i+1/2}$ is simply given by

$$\hat{q}_{i+1/2} = q_i + \frac{1}{2}\left(1 - \frac{U_{i+1/2}}{m_i}\right)(\delta q)_i \quad \text{if } U_{i+1/2} > 0 \tag{18}$$

$$= q_{i+1} - \frac{1}{2}\left(1 + \frac{U_{i+1/2}}{m_{i+1}}\right)(\delta q)_{i+1}\text{ , otherwise.} \tag{19}$$

In Van Leer scheme I, slopes are just estimated at each time step by finite differences ($\delta q_i = (q_{i+1} - q_{i-1})/2$).

In order to keep the monotonicity of q in region where q is monotonic (and thus to avoid the creation of negative values and spurious numerical oscillation as in many other schemes), Van-Leer (1977) showed that one sufficient requirement was that the entire dust distribution in a given mesh i does not exceed the mean value in the two adjacent boxes and that the slope must be of the same sign of that in the two adjacent boxes. In practice, we formulated this requirement by using a slope "limitation" :

$$(\delta q)_i = \text{sign}\,(q_{i+1} - q_i) \times \min\left(\frac{|q_{i+1} - q_{i-1}|}{2}, 2|q_{i+1} - q_i|, 2|q_i - q_{i-1}|\right) \tag{20}$$

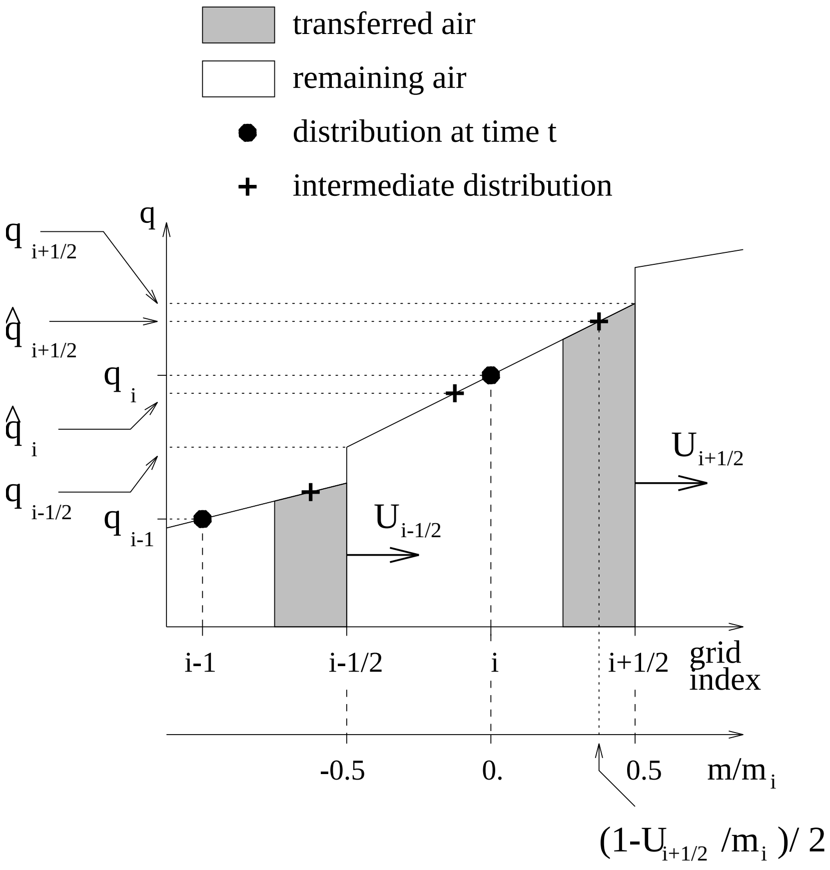

Figure 1: *Principle of Van Leer 1 finite volume schemes and notations. The vertical axis corresponds to the dust mixing ratio. The horizontal axis is shown both for grid index and for the mass counted from the center of mesh i and normalized by the mass of this mesh (m_i). The shaded areas correspond to the quantity of dust which is advected through the mesh interfaces during one time step.*

if q_i lies in between q_{i-1} and q_{i+1} and

$$(\delta q)_i = 0 \tag{21}$$

otherwise.'

4.1.2 *Implementation in the GCM*

The numerical implementation of finite volume schemes is particularly easy in the LMD GCM since mass fluxes are already defined at the mesh interfaces (C-grid) and used to solve the continuity equations which guaranties a complete consistency between dust and mass advection.

Time splitting. The adaptation to 3-Dimensional grid is based on time splitting : advection is done sequentially in the 3 directions.

We adopted the sequence proposed by Russel and Lerner(1981) :

Direction	time step
X	$\delta t/2$
Y	$\delta t/2$
Z	δt
Y	$\delta t/2$
X	$\delta t/2$

For each step, the values of both mass and dust mixing ratio are updated following Eq. 17 and Eq. 16.

Advection over more than one mesh in one time-step. The refinement of the longitudinal discretization near the poles for longitude latitude grids requires smaller and smaller time steps if one wants to satisfy the criterion that $U < m$. To avoid this problem, we took advantage of the fact that advection can be computed exactly for $U = m$. For $U > 0$, to fix idea, and if $U_{i+1/2} > m_i$, the distribution is shifted by n meshes where n is defined by

$$\sum_{j=i-n+1}^{i} m_j < U_{i+1/2} \leq \sum_{j=i-n}^{i} m_j \tag{22}$$

before applying the previous scheme. This leads to

$$F_{i+1/2} = \sum_{j=i-n+1}^{i} m_j q_j + \left(U_{i+1/2} - \sum_{j=i-n+1}^{i} m_j \right) \hat{q}_{i-n+1/2} \tag{23}$$

with

$$\hat{q}_{i-n+1/2} = q_{i-n} + \frac{1}{2} \left(1 - \frac{U_{i+1/2} - \sum_{j=i-n+1}^{i} m_j}{m_{i-n}} \right) \tag{24}$$

Polar discretization. In the LMD GCM, the poles correspond to a mesh center, with the horizontal mesh twice smaller than current meshes in the meridional direction. The model uses a unique value of the mass and other scalar fields at the pole. The time evolution of the mass is computed from the integrated meridional mass fluxes over all the meshes around the pole.

The same scheme was retained for the dust advection. However, no way of insuring strict monotonicity at the pole was found except by using zero slopes. Thus the scheme is equivalent to Godunov's (upstream) at the pole.

4.2 Performance and test

The transport scheme described here has been tested carefully in the Terrestrial GCM an some tests have already been done with the martian GCM. Analysis made with realistics wind fields are available in Hourdin and Armengaud (1997). Nevertheless, to illustrate the performance of the chosen scheme and justify our choice, we present below a a test of horizontal advection with a simple analytical wind field for which the advection can also be computed analytically.

The performance of the Van-Leer I scheme are compared to higher order transport schemes (based on a polynomial approximation to the subgrid scale tracer distribution in the upstream volume). These schemes are the "slopes scheme" (Russel and Lerner, 1981) which is, in fact, quite similar to the Van-Leer I scheme but in which the slopes (first order moment) are conserved during advection, and the "Prather's scheme" (Prather 1986), in which first and second order moments are conserved during advection. The Prather scheme is now considered as a reference in the GCM community.

2-Dimensional tests

For a non diverging horizontal flow in the longitude-latitude (λ, ϕ) reference frame, the zonal (u) and meridional (v) wind components satisfy the following relation:

$$\frac{\partial u}{\partial \lambda} + \frac{\partial v \cos\phi}{\partial \phi} = 0 \tag{25}$$

The analytical wind field used for advection is derived from the following poten tial

$$\Psi = aU_0 \cos^2 \frac{\lambda}{2} \cos^2 \phi \tag{26}$$

(where U_0 is a normalizing velocity and a the planetary radius) as

$$u = \frac{1}{a}\frac{\partial \Psi}{\partial \phi} = -2U_0 \cos\phi \sin\phi \; cos^2(\frac{\lambda}{2} \tag{27}$$

$$v = \frac{1}{a\cos\phi}\frac{\partial\Psi}{\partial\lambda} = -U_0\cos\phi\cos\frac{\lambda}{2}\sin\frac{\lambda}{2} v = \frac{1}{a\cos\phi}\frac{\partial\Psi}{\partial\lambda} = -U_0\cos\phi\cos\frac{\lambda}{2}\sin\frac{\lambda}{2} \tag{28}$$

Following a trajectory (constant value of Ψ) the meridional velocity $v = a\mathrm{d}\phi/\mathrm{d}t$ can be rewritten by combining Eq. 26 and Eq. 28 as

$$a\mathrm{d}\phi/\mathrm{d}t = -\sqrt{\Psi U_0/a}\ \mathrm{sign}\lambda\sqrt{1-\cos^2(\lambda/2)} \tag{29}$$

By introducing $\alpha = \sqrt{\Psi U_0/a^3}$ and after replacing $\cos^2(\lambda/2)$ according to Eq. 26, this equation can be integrated as

$$\begin{aligned} -\alpha\int \mathrm{sign}\lambda\mathrm{d}t &= \int\frac{\cos\phi\mathrm{d}\phi}{\sqrt{\cos^2\phi - \Psi/(aU_0)}} \\ &= \left[\arcsin\left(\frac{\sin\phi}{\sqrt{1-\Psi/(aU_0)}}\right)\right] \end{aligned} \tag{30}$$

The trajectories correspond to iso-values of Ψ. The time law is that given above. The time taken by an air parcel to come back to its original position is $2\pi/\alpha = 2\pi a/(U_0\cos\phi\cos\lambda/2)$. This period it shorter at the center of the domain and infinite on the boundaries.

For the numerical tests, the time step was chosen small enough to avoid the problem of near polar advection for the Prather's and Slopes schemes for which the special treatment in longitude described above is not implemented. In practice, the length of the simulation was fixed in order to have a full rotation at the center of the domain. The total number of time-steps is 4000, 6000 and 12000 for increasing resolutions. Note that a change of time step modifies the accuracy of the results but much less than a change of resolution.

The winds are shown in the upper left corner in Fig. 2 with an arbitrary scale as well as the initial distribution chosen for numerical tests : a gaussian in longitude constant on the vertical. The two panels on the right show successive distributions computed analytically from the formula above. The air rotates faster near the center of the figure than close to the boundary which produces a spiral.

The very accurate reconstruction of the fine central filament (values larger than 0.9) by the Prather's scheme for the full resolution is of course very impressive. However, the Slopes scheme does as well or even somewhat better for the full resolution than Prather's scheme in half resolution. Same thing between Van Leer scheme I on the full grid and the slope scheme in low resolution.

So, for the impact of changing the resolution in two directions only, Van Leer scheme I is somewhat better than Slopes and Slopes better than Prather's. When changing the resolution in the three directions, the comparison must be made between the high and intermediate resolution with a significant advantage for Prather's with respect to Slopes or Slopes with respect to Van Leer I.

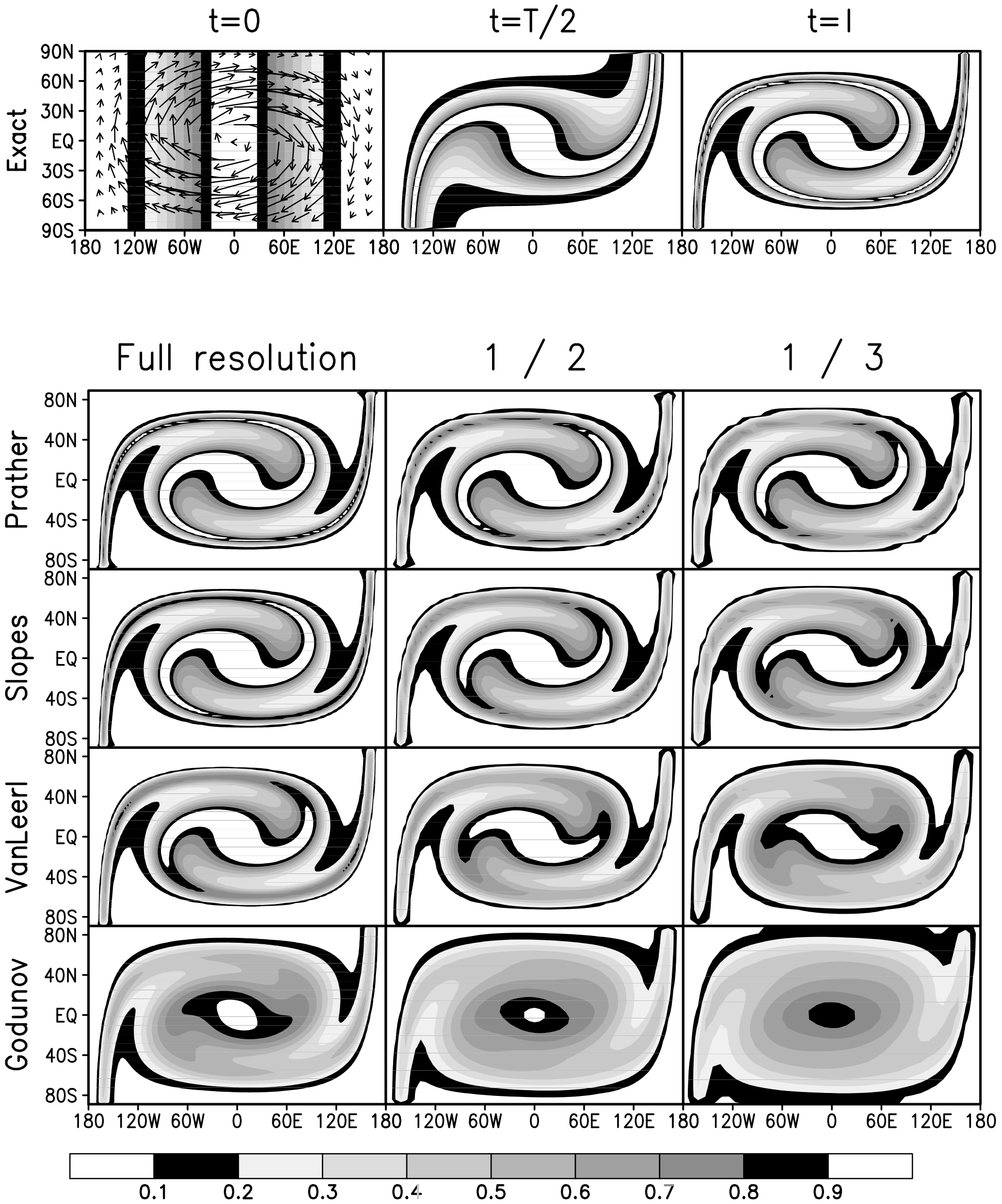

Figure 2: Performance of the Van-Leer I transport scheme chosen for our parametrisation of the martian dust, compared to other schemes and an analytical solution (horizontal advection with an analytical wind field). The initial tracer distribution is a gaussian function of latitude only. The upper panel shows the tracer distribution at time zero, and at time $T/2$ and T as computed with the analytical solution. The lower panel shows the results at time T the result of advection with the different transport schemes for various resolutions (full resolution with 120×60 points, 1/2 with 60×30 and 1/3 with 40×20 in longitude-latitude.

Note also the large difference in performance between the Godunov scheme and Van Leer I despite of their equivalent storage requirement.

Tests conclusions

It appears that the schemes are very comparable one to another when compared at different spatial resolutions in order to make their relative numerical cost comparable. If neutral in terms of performances on pure advection, the comparison is much more favorable to Van Leer scheme I for practical applications. The reason is the difficulty of accounting for the effect on higher order moments of the distribution for other processes (lifting. sedimentation) which must be accounted for in physical applications.

The numerical properties of the 3-Dimensional implementation used in the LMD model are summarized below.

- The scheme is conservative.
- It is monotonic preventing the creation of negative values and spurious numerical oscillations.
- It doesn't modify a constant tracer field, and that independently of the wind field.

5 Dust deposition

5.1 Gravitational sedimentation

Because of their higher density relative to air, dust particles fall down by gravity. The corresponding downward transfer of dust is computed separately from the transport, but using a similar Van-Leer I scheme. In practice, we used Eq. 16 in the vertical dimension, with $m_i^* = m_i$ (the air masses of the layers are, of course, not changed during this process), and with U the mass "transfer" corresponding to the sedimentation velocity of the dust particle W_s. The fact that the dust particles may fall through more than one time step is accounted for by using equations deduced from Eq. 22.

W_s is computed using the Stokes law corrected for low pressure by the Cunningham slip-flow correction (Rossow, 1978):

$$W_s = \frac{2}{9} \frac{\rho_d \, g}{\mu} \, r^2 (1 + \frac{4}{3} \frac{\lambda}{r}) \tag{31}$$

where μ is the gas molecular viscosity ($\mu \simeq 10^{-5}$ N s m^{-2} for CO_2 in martian conditions), ρ_d the dust particle density ($\rho_d \simeq 2700$ kg m^{-3}), r the particle radius($r \sim 1\mu$m), and λ the gas mean free path (m). For CO_2 gas (molecular radius of 2.2×10^{-10} m), λ is given by :

$$\lambda = 1.6 \times 10^{-5}\, \frac{T}{p} \tag{32}$$

where p is pressure and T temperature.

Particles can fall "through" the surface. They are then removed from the atmosphere (deposition). The amount of dust which is deposited in each grid point is kept in memory for information.

5.2 Turbulent diffusion to surface

Very near the surface, in a region refferred to as the interface layer, surface deposition occurs (in addition to gravitational sedimentation) through various mechanisms, depending on the particle size (Jousseaume 1990): Brownian diffusion for very small particles ($< 0.1\mu$m) or for molecules ; interception by obstacles (particles larger than 0.1 μm), a phenomenon which increases with the size of the particles as their trajectories deviate from streamlines by reason of their inertia ("impaction").

To account for these phenomenons, we have assumed that the dust reaching the surface due to turbulent mixing was lost when no dust lifting was occuring. In practice, this process is taken into account in the vertical diffusion scheme. The corresponding sink of dust from the first layer to the surface is

$$\frac{\partial q(1)}{\partial t} = -\frac{g}{\delta\sigma_1 p_s}\, \rho\, C_d\, u(z_1)\, q(1) \tag{33}$$

with the same notations as in section 2.1.

6 Deposition due to condensation

6.1 CO_2 condensation in the winter polar regions

According to basic microphysical considerations, it is very likely that, in the winter polar atmosphere , CO_2 ice condenses on the airborne dust particles. Not only dust particles are likely condensation nuclei (heterogeneous condensation), but, because of their high emissivity compared to CO_2 gas, they should radiatively cool more rapidly than the surrounding atmosphere. It is thus likely that each "flakes" of CO_2 ice that have condensed in the atmosphere contains at least one dust particle.

Doing so, atmospheric CO_2 condensation should accelerate dust removal (scavenging). The winter polar regions could thus be a major sink of dust that have to be taken into account.

On Earth, similar processes occur in water clouds and they are though to control dust removal (Slinn, 1983). However, the physical processes involved are very complex and poorly known (cf. Pruppacher and Klett, 1978). Parametrizing this process on Mars in CO_2 clouds is thus extremely difficult. Nevertheless, we have designed a very simple scheme to take this process into account.

In theory, dust can be "washed out" during the condensation phase (nucleation scavenging) or during the fall of the ice flakes (collision scavenging). On Earth, it is usually considered that this last process is negligible when the dust particles are small compared to to the condensed particles. On Mars, this distinction is somewhat artificial since condensation occurs at every level (and not in a cloud layer as on Earth). Therefore, we have assumed that collision scavenging is negligible, or, in fact, that it is taken into account in the simple nucleation scavenging parametrization.

Following numerous terrestrial parametrization for water clouds, (e.g. Joussaume, 1990), we have assumed that, during condensation, the amount of dust included in the precipitation is proportional to the local dust mixing ratio. Thus, we have introduced a "Scavenging ratio" $\mathcal{R}$:

$$\mathcal{R} = \frac{\text{Dust mixing ratio in ice}}{\text{Dust mixing ratio in the atmosphere}} \tag{34}$$

In a given mesh of the model, the condensation rate in a layer l of mass per surface unit M_l (kg m^{-2}) is $\partial m_l/\partial t$ (kg m^{-2} s^{-1}, > 0 when condensing). This layer contains the mass $M_{\mathrm{dust(l)}} = q_l M_l$. $\mathcal{R}$ can be written:

$$\begin{aligned}\mathcal{R} &= (\frac{-\partial M_{\mathrm{dust(l)}}/\partial t}{\partial m_l/\partial t})\,(\frac{1}{q_l}) \\ &= \frac{-1}{q_l}\,\frac{\partial q_l}{\partial t}\,(\frac{\partial m_l}{\partial t})^{-1}\,M_l\end{aligned} \tag{35}$$

This gives the governing equation for dust scavenging :

$$\frac{\partial q_l}{\partial t} = -\mathcal{R}\,q_l\,\frac{\partial m_l}{\partial t}\,\frac{1}{M_l} \tag{36}$$

Integration over one timestep δt gives the increment for q at each model timestep :

$$\delta q_l = -\tau[1 - \exp(-\frac{\mathcal{R}}{M_l}\delta m_l)] \quad (37)$$

This simple parametrisation only depends on the scavenging ratio $\mathcal{R}$. Can we estimate it ? On Earth, this ratio can be estimated almost directly during observations campaigns. Slinn (1983) reports values of the order of 10^2-10^3 in convective clouds. As for Mars, if one assume that the size of the CO_2 ice "flakes" is of the order of 100μm (Wood et al., 1996), a simple calculation[1] shows that the number of dust particles of radius 2 μm included in each ice flake should be around $N \simeq \mathcal{R}\tau$, with τ the total atmospheric visible optical depth. N should be at least 1, and probably much more. $\mathcal{R}$ should thus range between 1 and 100, maybe more.

Preliminary studies performed with this simple parametrisation using a simple restoring function to account for the transport of dust in the polar region indicate that this process should be very efficient to remove dust in the polar region, even for low value of $\mathcal{R}$ (Forget, 1996).

6.2 Water ice condensation

As shown by Michelangeli et al. (1993) and previous microphysical models of Mars water ice clouds, the condensation of high altitude water ice around dust may also lead to rapid gravitational settling, and, hence, cleansing of dust from the Mars upper atmospgere (> 25 km). The removal of the dust leads to cooling of the atmosphere such that the altitude of water saturation/ice cloud formation is propagated downward. This highly non-linear dust-ice-temperature fedback has been argued to account for the strong temporal variations of Mars dust loading and atmospheric temperature (Clancy et al., 1996).

Modeling such an effect should thus be of interest for our model. However, it requires a more or less complex parametrization of the martian water cycle which is not yet simulated in our model. nevertheless, A preliminary design of this effect may be included in the model in the future.

[1]In the martian atmosphere, the dust optical depth τ is proportional to the total mass of airborne dust : $M_{\text{pous}} \simeq \tau/500 \quad (\text{kg.m}^{-2})$ (Martin, 1995) The corresponding dust mixing ratio is $Q_{\text{atm}} = \tau g/500 p_0$ with $p_0 \simeq 500$ Pa surface pressure. In the CO_2 ice flake of radius $r_{\text{ice}} = 100$ μm, the dust mixing ratio of N dust particles included in the flake is : $Q_{\text{ice}} = N(\rho_{\text{dust}} r_{\text{dust}}^3)/(\rho_{\text{ice}} r_{\text{ice}}^3)$ (using ρ_{ice} =1620 kg.m^{-3} and ρ_{dust} =2700 kg.m^{-3} The corresponding scavenging ratio is $\mathcal{R} = Q_{\text{ice}}/Q_{\text{atm}} \simeq N/\tau$

References

[Arvidson et al.(1983)] Arvidson, R., E. A. Guiness, H. Moore, J. Tillman, and S. Wall, 1983, Three Mars years: Viking Lander 1 imaging observations, *Science*, *222*, 463–468, 1983.

[Clancy et al.(1996)] Clancy, R., A. W. Grossman, M. J. Wolff, P. B. James, D. J. Rudy, Y. N. Billawala, B. J. Sandor, S. W. Lee, and D. O. Muhleman, 1996, Water vapor saturation at low altitudes around Mars aphelion: a key to Mars climate, *Icarus*, *122*, 36–62, 1996.

[Forget(1996)] Forget, F., *Le climat de la planète Mars : de l'importance des poussières et des régions polaires.*, thèse, Université Paris-6, 1996.

[Greeley et al.(1980)] Greeley, R., L. R., B. White, J. Iversen, and J. Pollack, 1980, Threshold windspeeds for sands on Mars: wind tunnel simulations, *Geophys. Res. Lett.*, *7*, 121–124, 1980.

[Greeley et al.(1994a)] Greeley, R., D. G. Blumberg, and S. H. Williams, Field measurements of active windblown sand, Abstract of the workshop on Reponse of Eolian Processes to Global changes, Desert research Institute, 1994*a*.

[Greeley et al.(1994b)] Greeley, R., M. Lacchia, B. White, R. Leach, D. Trilling, and J. Pollack, Dust on Mars: new values for wind threshold, in *XXV Lunar Planet. Sci. Conf.*, 467–468, 1994*b*.

[Hourdin and Armengaud(1997)] Hourdin, F., and A. Armengaud, 1997, Test of a hierarchy of finite-volume schemes for transport of trace species in an atmospheric general circulation model, *submitted to Monthly Wheather Review*, 1997.

[Joussaume(1990)] Joussaume, S., 1990, Three-dimensional simulations od the atmospheric cycle of desert dust particles using a general circulation model, *J. Geophys. Res.*, *95*, 1909–1941, 1990.

[Marticorena and Bergametti(1995)] Marticorena, N., and G. Bergametti, 1995, Modeling the atmospheric dust cycle: design of a soil-derived emission scheme, *J. Geophys. Res.*, *102*, 16,415–16,430, 1995.

[Martin(1995)] Martin, T. Z., 1995, Mass of dust in the martian atmosphere, *J. Geophys. Res.*, *100*, 7509–7512, 1995.

[Michelangeli et al.(1993)] Michelangeli, D. V., O. B. Toon, R. M. Haberle, and J. B. Pollack, 1993, Numerical simulations of the formation and evolution of water ice clouds in the Martian atmosphere., *Icarus*, *100*, 261–285, 1993.

[Prather(1986)] Prather, M. J., 1986, Numerical advection by conservation of second order moments, *J. Geophys. Res.*, *91*, 6671–6681, 1986.

[Pruppacher and Klett(1978)] Pruppacher, H. R., and J. D. Klett, *Microphysics of clouds and precipitation*, D. Reidel, 1978.

[Rossow(1978)] Rossow, W. B., 1978, Cloud microphysics: Analysis of the clouds of Earth, Venus, Mars, and Jupiter, *Icarus*, *36*, 1,50, 1978.

[Russel and Lerner(1981)] Russel, G. L., and J. A. Lerner, 1981, A new finite-differencing scheme for the tracer transport equation, *J. Appl. Met.*, *20*, 1483–1498, 1981.

[Ryan and Lucich(1983)] Ryan, J. A., and R. D. Lucich, 1983, Possible dust devils vortices on Mars, *J. Geophys. Res.*, *1983*, 11005–11011, 1983.

[Shao et al.(1993)] Shao, Y., M. R. Raupach, and P. A. Findlater, 1993, Effect of saltation bombardment on the entrainment of dust by wind, *J. Geophys. Res.*, *98*, 12719–12726, 1993.

[Slinn(1983)] Slinn, W. G. N., Air to sea transfer of particles, in *Air -sea exchange of gases and particles*, edited by P. Liss and W. G. N. Slinn, 299–405, D. Reidel Publishing Company, 1983.

[Thomas and Gierasch(1985)] Thomas, P., and P. J. Gierasch, 1985, Dust devils on Mars, *Science*, *230*, 175–177, 1985.

[Van Leer(1977)] Van Leer, B., 1977, Towards the ultimate conservative difference scheme : IV. a new approach to numerical convection, *J. Computational Phys.*, *23*, 276–299, 1977.

[White and Greeley(1989)] White, B. R., and R. Greeley, Martian dust threshold measurements: simulation under heated surface conditions, in *MECA Workshop on dust on Mars III*, edited by S. Lee, number 89-01, 60–61, L.P.I Tech. Rept., 1989.

[White(1979)] White, B. R., 1979, Soil transport by winds on Mars, *J. Geophys. Res.*, *84*, 4643–4651, 1979.

[Wood et al.(1996)] Wood, S. E., M. I. Richardson, and D. A. Paige, 1996, A microphysical model of CO_2 snow on Mars, *Bull. Am. Astron. Soc.*, *28*, 1065, 1996.